4

Regional Climate Variability and Extremes: Challenges for Adaptation

4

Regional Climate Variability and Extremes: Challenges for Adaptation

4.1

Introduction

Climate change mitigation goals, such as deep decarbonization by 2050, play a central role in the development of climate futures. However, a crucial yet under-researched reason for climate change impacts and adaptation challenges lies in the effect of internal climate variability, which arises spontaneously in the coupled climate system (Section 4.2), and in particular in how extreme weather events „ride" on the tails of statistical distributions. The issue is perhaps best illustrated by an example. It is well known that storm surges tend to become more severe when they occur on top of rising mean sea level (e.g., Fox-Kemper et al., 2021, WGI AR6 Chapter 9). Similarly, the entire statistical distribution of summer temperatures shifts toward higher values with mean climate warming, implying warmer extremes (e.g., Suárez-Gutiérrez et al., 2018). By contrast, it appears to be less appreciated that the occurrence of the extremes themselves not only follows the long-term climate change but shows internal climate variability on interannual to decadal timescales, meaning that the frequency of extreme events might go up one decade but decrease during the next, against the backdrop of an overall increase with global warming. As an example of this lack of appreciation, the IPCC Special Report on Global Warming of 1.5°C (IPCC SR1.5, 2018) mentioned internal climate variability quite a few times but did not offer a single quantitative analysis.

However, we showed in the 2021 Outlook edition (Marotzke et al., 2021; based on Suarez-Gutierrez et al., 2018) that worlds differing by 0.5°C in decadal global surface temperature show hotter extremes in the warmer world but also substantial overlap in possible extreme European summer temperatures. This overlap is a manifestation of internal climate variability, defined loosely as those variations in climate that "simply occur" with no apparent cause (Section 4.2). Suárez-Gutiérrez et al. (2023) show another important effect of decadal internal climate variability: Events currently considered extreme and expected to be normal by 2100 in a warming climate will become plausible already in the coming two decades. By "plausible" we mean here that the events will happen with appreciable probability; whether an event will indeed occur depends not only on the future evolution of global warming but also on chance. This role of chance (technically described as aleatoric uncertainty) contrasts with the dominant expectation that a decadal change in extremes is solely due to anthropogenic effects (e.g., Christidis et al., 2015), whereas what is observed actually shows a combination of anthropogenic effects and natural variability.

Knowledge of regional variability and extreme events is a crucial ingredient when trying to deal with climate change adaptation, which must prepare for extremes no matter what their cause. Global warming exacerbates many extremes, but on the regional or local scale the distribution of internal climate variability is often wider than the anthropogenic effect (e.g., Lee et al., 2021, WGI AR6 Chapter 4). "Regional climate change and variability" was one of the six physical processes analyzed in the previous Outlook (Sillmann, 2023). We addressed physical processes that determine regional climate variability and the role of climate variability in amplifying or attenuating changes in climate extremes on a regional scale. We further explained how global warming plays out differently on the regional scale due to climate variability and regional processes. Here we follow up on that assessment and establish regional climate variability and extremes as physical boundary conditions to the overarching question of the current Outlook: Under which conditions is sustainable climate change adaptation plausible? The physical boundary conditions set the room to maneuver both for mitigation and adaptation.

The interplay of regional variability and extremes poses a particular challenge to sustainable adaptation to climate change as assessed in Chapter 5. The sequence of examples discussed in the

subsequent sections of this chapter represents an eclectic ensemble of opportunities. Each is based on very recent research and can thus claim some newsworthiness; but each also illustrates a particular fundamental point relevant for the plausibility of sustainable climate change adaptation: the capability of climate models to represent extremes (here: precipitation), the attribution of extreme events to human influence (here: marine heatwaves), and the probability of compounding extreme events (here: extreme heat in multiple breadbasket regions). While each example thus features strong reasons for inclusion here, we do not claim comprehensive coverage of the interplay of regional variability and extremes—hence the rather modest characterization of our set of examples as "eclectic".

Many examples of local manifestations relevant for sustainable adaptation challenges covered in Chapter 5 had to be left out here but hopefully can be covered in future editions. However, along the way and where appropriate we foreshadow the relevance of the physical processes and results for the adaption challenges that are assessed in Chapter 5. The Max Planck Institute Grand Ensemble (MPI-GE, Section 4.2; Maher et al., 2019) contributes to shaping international research on internal climate variability. New ensemble runs comprising 30 realizations with updated scenarios and much-enhanced output now enable us to analyze the interplay of internal climate variability and extreme events.

We explain in greater detail the concept of internal climate variability, how the new MPI-GE contribution was constructed, and what it can provide (Section 4.2). Section 4.3 investigates the extent to which the MPI-GE is able to represent precipitation extremes. This section gives insights into climate model capabilities and limitations, which is important information for the development of adaptation strategies. Section 4.4 analyzes marine heatwaves and the extent to which they can be attributed to human influence. Section 4.5 considers temporal compounding extreme events, here understood regionally in that the section investigates the probability of multiple breadbasket regions experiencing extreme heat simultaneously, also addressing implications for society.

4.2

Single-Model Initial-Condition Large Ensembles Quantify Internal Climate Variability and its Changes

Internal climate variability arises from the chaotic interactions within and between components of the climate system such as atmosphere, ocean, cryosphere, and land (e.g., Lee et al., 2021, WGI AR6 Chapter 4). The existence of internal climate variability potentially obscures signals in the climate system. For instance, internal climate variability impacts the global warming signal, leading to temporary acceleration, slowing down, or even reversal of global warming (e.g., Hedemann et al., 2017; Marotzke, 2019). These impacts on climate trends and variations act on global, regional, and local spatial scales, and on sub-daily to multidecadal and longer time scales (e.g., Maher et al., 2021). This makes understanding and projecting internal climate variability challenging. Specific tools to address this challenge are required. Single-model initial-condition large ensembles, hereafter just called large ensembles, are one such tool (Deser et al., 2020; Figure 4.1).

Large ensembles substantially improve the understanding and quantification of climate variability and change. The underlying idea is to sample the internal climate variability of the climate system by running the same climate model multiple times with slightly different initial conditions but the same external forcing, such as changes in atmospheric greenhouse gas concentrations from human-caused emissions or volcanic eruptions. The different initial conditions of each simulation create different climate trajectories that cause the simulations to diverge quickly, forming a spread of possible climates (Figure 4.1). The simulations are either started from different times of a pre-industrial control simulation (as in Figure 4.1) or from the same coupled model state but with slight perturbations at the level of round-off errors in the atmosphere or ocean at the start of each simulation. Any single ensemble member represents one conceivable evolution of the climate system, taking both external forcing scenarios and internal variability into account. This practice addresses the chaotic evolution of the climate system. The resulting set of simulations is called an ensemble. Ensembles may come in different forms and sizes, depending

on the intended purpose. An ensemble is commonly named as "large" when the ensemble size is at least 30 (Milinski et al., 2020).

Large ensembles have enabled substantial progress in understanding the Earth system. They have been used to separate, with unprecedented precision, internal climate variability from the forced response of the climate system to external forcing. This was done to evaluate how well climate models capture the variability and forced changes in the historical observational record (Maher et al., 2019; Olonscheck et al., 2021; Suárez-Gutiérrez et al., 2021). This allows quantifying changes in the magnitude and spatial structure of climate variability related to global warming (Figure 4.1, global maps 1-7). Large ensembles have also been used to identify systematic differences between simulated and observed patterns of sea-surface temperature and sea-level pressure change, indicating which parts of the patterns are unlikely to occur due to internal variability alone (e.g., Olonscheck et al., 2020; Wills et al., 2022). Furthermore, recent developments in compound-event research, that is, the research on the occurrence of several extreme events at the same time, in close proximity (spatial compounding) and/or in quick succession (temporal compounding), highlight the importance of sufficiently sampling internal climate variability to robustly capture this type of extreme (Zscheischler et al., 2022; Section 4.5). Capturing compound events requires even larger ensemble sizes than univariate extremes (Bevacqua et al., 2023). The availability of large ensembles from multiple different global climate models further allows us to account for inter-model differences in their climate response.

Overall, large ensembles allow for a better quantification and differentiation between three main sources of uncertainties in present and future climate (Hawkins and Sutton, 2009; 2011; Deser et al., 2020; Lehner et al., 2020; Lee et al., 2021):

1. Uncertainty from internal variability: This uncertainty arises from the inherent chaotic nature of the climate system. Since some climate variations occur naturally due to this chaotic nature of the system, it is important to understand which portion of the diagnosed climate change is forced and which is internally generated. Sampling the full range of internal climate variability and their changes is therefore paramount for understanding, attributing, and projecting climate change (Jain et al., 2023). The uncertainty from internal variability is irreducible, making the exact evolution of the climate system unpredictable, no matter how much we understand about the system (Lorenz, 1963; Hawkins et al., 2016; Marotzke, 2019; Lehner et al., 2020). Large ensembles allow us to quantify this uncertainty in a climate model at better precision than ever before, and—importantly—also to quantify how internal climate variability might change over time under external forcing (Brown et al., 2017; Maher et al., 2018; Olonscheck et al., 2021). This is possible by quantifying the ensemble spread of the simulations at every time step, including projected future times. Since large ensembles are set up such that their spread covers observed climate system variability during the historical period, they represent this type of uncertainty to the best possible extent (e.g., Maher et al., 2018). Large ensembles also allow for an accurate quantification of the externally forced climate response. This forced climate response is represented by the ensemble mean. The ensemble mean is derived from averaging over all simulations for the historical period or one future scenario (Figure 4.1), which cancels out the internal climate variability.
2. Model structural uncertainty: This uncertainty arises from structural differences between models in their imperfect mathematical and physical description of the climate and in how the models respond to external forcing as is commonly shown in IPCC-type climate projections (Lee et al., 2021, WGI AR6 Chapter 4, their Figure 4.2). For example, differences in model resolution or their parameterization of sub-grid scale processes fall into this category (Section 4.3). As such, this uncertainty is reducible by improving how climate models describe the Earth system. Large ensembles from multiple global climate models allow us to quantify the uncertainty from structural differences of climate models in the light of the irreducible uncertainty arising from internal climate variability. A robust estimate of the forced climate response as provided by large ensembles is therefore required to precisely distinguish model structural uncertainty from internal climate variability.
3. Scenario uncertainty: This uncertainty is caused by our imperfect knowledge of how society will behave in the future, and primarily how this behavior reflects in the amount of future greenhouse gas emissions (Figure 4.1). Emissions scenarios are possible future pathways that cover different manifestations of future climates under the assumption of socio-economic decisions, the so-called shared socio-economic pathways (SSP, Riahi et al., 2017; Lehner et al., 2023). The scenario uncertainty is represented by different pathways of the greenhouse gas, aerosol, and land use change forcings to the climate system that may occur under different socio-economic assumptions. This uncertainty is considered irreducible from a natural climate science perspective. Here in the current Outlook we have assessed that the highest and the lowest SSP scenarios (Riahi et al., 2017) are not plausible (Stammer et al., 2021; Engels et al., 2023). The choice of the SSP emissions scenario governs a substantial portion of the magnitude of end-of-century climate change, as illustrated by the large differences in mean surface air temperature in the year 2100 between scenarios.

We here introduce the large ensemble that is most frequently used in this chapter: The Max Planck Institute Grand Ensemble in its so-called CMIP6 version (hereafter MPI-GE CMIP6, Olonscheck et al., 2023). This ensemble is run with the Max Planck Institute Earth System Model (MPI-ESM1.2-LR, Mauritsen et al., 2019). MPI-GE CMIP6 has 30 historical simulations covering the period from 1850 to 2014 and 30 simulations for five future emissions scenarios from 2015 to 2100 (Riahi et al., 2017). Thirty ensemble members are a sufficient ensemble size to adequately estimate the uncertainty of most climate variables (Milinski et al., 2020). The low-emission scenario SSP1-1.9 is in line with the goal to limit global warming to 1.5°C, whereas the high-emission scenario SSP5-8.5 represents a world almost 5°C warmer by 2100 compared to the second half of the 19th century. The possible future climates between SSP1-1.9 and SSP5-8.5 are sampled in the three additional scenarios SSP1-2.6, SSP2-4.5, and SSP3-7.0.

The predecessor ensemble MPI-GE CMIP5, consisting of 100 simulations and with a monthly output, adequately sampled observed internal variability in temperature (Maher et al., 2019; Suárez-Gutiérrez et al., 2021). The 30 simulations with 3-hourly to daily output of MPI-GE CMIP6 in addition sample a large number of extreme events (Olonscheck et al., 2023). Since extremes are both rare by definition and strongly impacted by internal climate variability, an adequate sampling of internal climate variability is an important enabler of the study of extreme events (Suárez-Gutiérrez et al., 2021; Bevacqua et al., 2023). MPI-GE CMIP6 provides daily output for every parameter and output every three hours and every six hours for some key parameters. This high-frequency model output is central for capturing both short-lived extreme events, such as precipitation extremes, and the strongest intensities of other types of events such as heatwaves and storms (Olonscheck et al., 2023). MPI-GE CMIP6 is therefore suited to investigate short-lived, large-scale climate extremes. Another large ensemble that is used in Section 4.4 is CESM1-LE (Kay et al., 2015), operated by the National Center for Atmospheric Research in Boulder, Colorado, in the United States. CESM1-LE has similar capabilities to MPI-GE CMIP6 and provides single-forcing scenarios.

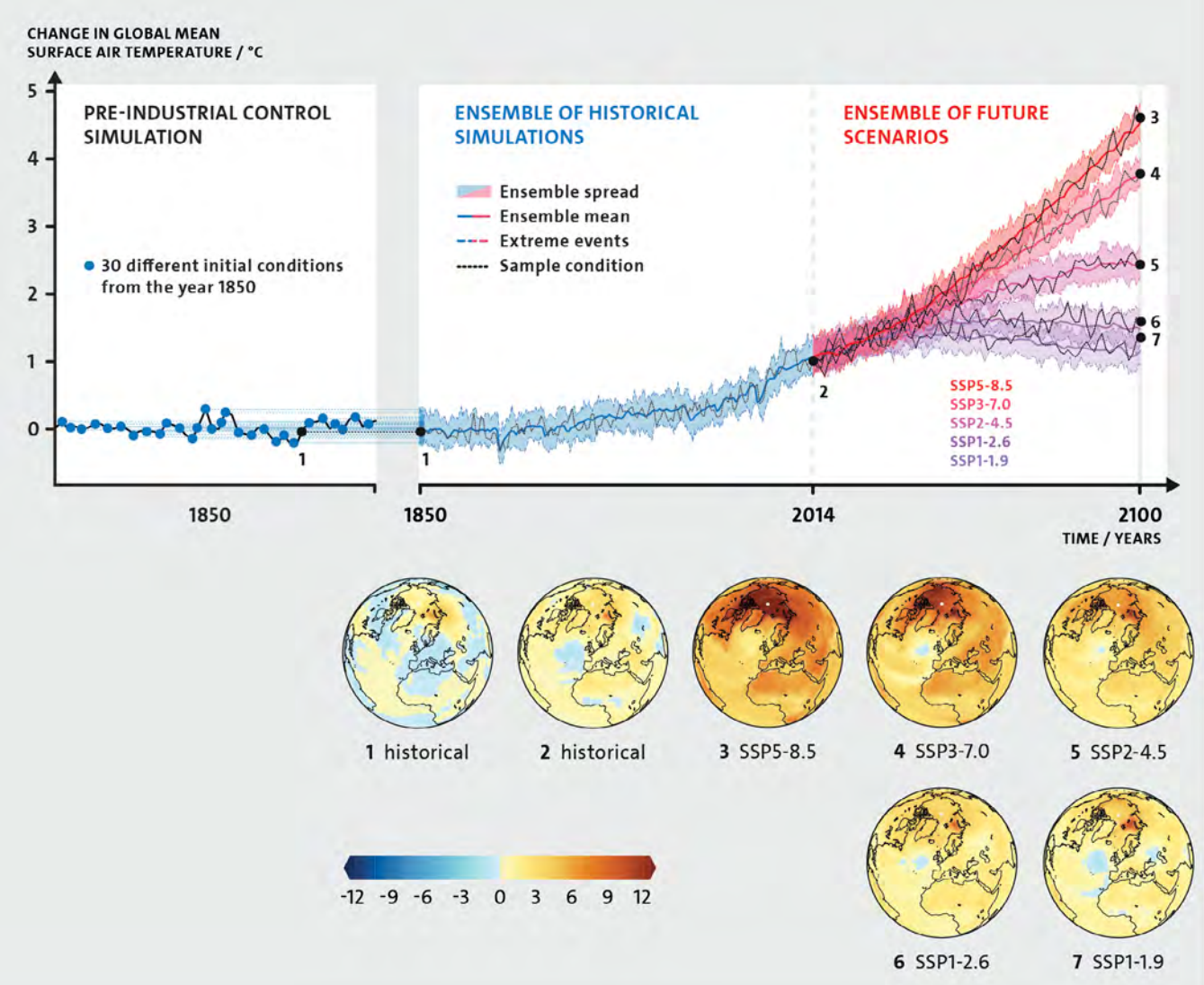

Figure 4.1: Schematic of the MPI-GE. Initial conditions (year 1850) for the 30 simulations are chosen from a pre-industrial control simulation and represent different conceivable climates for that year. The ensemble of 30 simulations for the historical period (1850-2014) span the possibility space of climate while considering internal variability (blue shading). The ensemble mean (blue line) estimates the forced response during that period. Five future scenarios (SSP1-1.9, SSP1-2.6, SSP2-4.5, SSP3-7.0 and SSP5-8.5) exist for all 30 ensemble members, covering the response of the climate system (red and purple lines), including uncertainty arising from internal variability (red-purple shadings). A single ensemble member is taken as an example (black line), starting from its own initial conditions in 1850 (1), which can be followed through the historical period (2) into five different futures, depending on the emission scenario (3-7). At different points in time, all ensemble members have their own climate state that represents a combination of forced response and internal variability. This is exemplified with the global temperature patterns from the first ensemble member shown at different points in time (global maps 1-7). The global maps 3-7 show the warming patterns in year 2100.

4.3

Are Recently Observed Heavy Precipitation Extremes Realistically Represented by State-of-the-Art Spatial Resolutions of Global Climate Models?

Precipitation extremes are among the most devastating events in terms of socio-ecological and economic losses, and their intensity and frequency are projected to increase with global warming, in part because warmer air can hold more water leading to increased precipitation intensity (Pendergrass et al., 2017; Myhre et al., 2019; Seneviratne et al., 2021; Thackeray et al., 2022). A global warming of 2°C would result in substantially more frequent heavy precipitation events than a global warming of 1.5°C, highlighting the potential to avoid substantial future increases in extreme precipitation by ambitious climate mitigation (e.g., Kharin et al., 2018). In addition to other risk determinants such as vulnerability, exposure, and local response measures, more intense precipitation extremes can significantly increase the risk of flooding and confront societies around the world with the challenge of adapting to the impacts of climate change to an even greater extent than is already required. Both rural and urban areas are affected by heavy precipitation extremes, but urban areas are particularly at risk of flooding due to their impermeable and sealed surfaces that do not retain water sufficiently (Revi et al., 2022; see also Sections 5.3 and 5.4). In addition, flooding risks are compounded by the location of settlements, with higher risks in cities located in low-lying areas and coastal zones (Dodman et al., 2022; see also Section 5.5).

In this section, we analyze how realistically the Max Planck Institute Grand Ensemble in its CMIP6 version (MPI-GE CMIP6, see Section 4.2) represents three recently observed record-shattering extreme events that impacted both rural and urban areas: the heavy precipitation extremes in western Europe on 14th July 2021, in the Western Alps on 2nd October 2020, and across the state of São Paulo, Brazil, on 10th February 2020. The extreme rainfall event on 14th July 2021 led to catastrophic flooding in western Europe, with urban areas along rivers of V-shaped notch valleys being particularly affected (Tradowsky et al., 2023). The heavy precipitation event over the Western Alps on 2nd October 2020 mainly affected south-eastern France and northern Italy and led to outages in electricity, telecommunications, water supply, and rail services, and also to significant infrastructure and environmental damages and at least 15 fatalities (Davolio et al., 2023). The heavy precipitation event on 10th February 2020 in the state of São Paulo, which hit São Paulo City during Carnival, a time when many tourists visit the city and many festivities take place, caused devastating floods, flash floods, and landslides that claimed dozens of lives and left thousands of people homeless (World Meteorological Organization, 2021; see also Section 5.4).

For the risk assessment, adaptation planning, and to evaluate what action is needed to address such challenges, robust and reliable local information on climate change is a prerequisite. The performance of climate models used to project future climate impacts is crucial to assess whether certain types of precipitation events (e.g., large-scale versus convective) will become more frequent or more intense over time. Therefore, we address the question: Do state-of-the-art global climate models capture recently observed extreme precipitation events?

Limits of state-of-the-art global climate models to simulate precipitation extremes

On top of significant biases in simulating mean precipitation, a realistic representation of observed heavy precipitation extremes by state-of-the-art global climate models is fundamentally limited because their simulations have 1) coarse spatial resolution (Slingo et al., 2022) and 2) substantial uncertainty from insufficiently sampling large internal climate variability (Deser et al., 2020). First, it is expected, and in part known, that higher spatial resolution of global climate models improves the simulation of extreme precipitation because higher-resolution models reflect smaller spatial scales and key processes such as atmospheric deep convection, and because ocean eddies are represented explicitly (Wehner et al., 2014; Iles et al., 2020; Kahraman et al., 2021; Kendon et al., 2021). Explicitly simulating how small and intermediate scales of motions couple to large-scale circulation systems, which allows us to circumvent problematic assumptions known as parameterizations, is expected to make a large difference at the kilometer scale

(Stevens et al., 2019; Slingo et al., 2022). However, kilometer-scale simulations are not yet available for multiple years or decades and so far do not allow for reasonable comparisons to observed climate trends. Second, properly characterizing internal climate variability is especially important for precipitation extremes. Increased precipitation variability can result in longer periods without precipitation and single heavy precipitation events. Extreme events are rare by definition, and robustly quantifying their occurrence substantially benefits from large sample sizes from many realizations, in particular at the local scale (Hawkins and Sutton, 2009; 2011).

Realism of simulating observed precipitation extremes – three case studies

To address the uncertainties from both internal climate variability and low spatial resolution, we use the MPI-GE CMIP6 (see Section 4.2) to adequately sample internal climate variability and to test whether higher resolution simulations of the same model version are better able to capture recently observed precipitation extremes in Europe than the low-resolution MPI-GE CMIP6. For this model evaluation, we focus on three events:

First, the extreme event in western Europe on 14th July 2021 (Figure 4.2, upper panel) that caused unprecedented flooding of the rivers Ahr and Erft and for which rapid attribution studies have shown high confidence that human-induced climate change has increased the likelihood and intensity of the events (Kreienkamp et al., 2021; Ibebuchi, 2022). The daily precipitation observed by the Europe-wide E-OBS data set (Klein Tank et al., 2002; Cornes et al., 2018) on 14th of July 2021 averaged across the western European domain is 47.7 mm, which represents the maximum daily precipitation in any summer during the 72-year long observed record. The extreme event was driven by an anomalously strong large-scale atmospheric circulation type with a mid-latitude cyclone over the North Sea and an anticyclone over the North Atlantic, enabling a band of westerly moisture fluxes to western Europe (Ibebuchi, 2022).

Second, the extreme event in the Western Alps on 2nd October 2020 (Figure 4.2, lower panel) caused devastating large-scale flooding and represents an unprecedented strong event in a region that shows a high frequency of precipitation extremes (Grazzini et al., 2021; Davolio et al., 2023). The daily precipitation observed by E-OBS on 2nd of October 2020 averaged across the domain in the Western Alps is 72.9 mm, the maximum daily precipitation in any autumn during the 72-year long observed record. This event was associated with an upper-level trough over the western Mediterranean basin, a large-scale pattern that is typical of heavy precipitation events on the southern side of the Alps, since it triggers a northward transport of large amounts of moisture interacting with the orography (Davolio et al., 2023).

Third, the extreme event across the state of São Paulo on 10th February 2020 (Figure 4.3). The daily precipitation of 123.0 mm/day on 10th February 2020 was the second-highest summer precipitation, surpassed only by the record-shattering event on 21st December 1988 with 151.8 mm/day (INMET, 2024). Marengo et al. (2020a) found that a significant increase in summer precipitation during the past 70 years is a key driver of increased risk, in association with precipitation-related hazards in São Paulo. This increase in heavy precipitation is at least partly caused by an intensification and southwestward propagation of the South Atlantic Subtropical Anticyclone that transports increased amounts of humidity to São Paulo City (Marengo et al., 2020b; see also Section 5.4).

We compare these observed events to simulations with three spatial model resolutions of MPI-ESM1.2. First, we use the 30 simulations of MPI-GE CMIP6 (Olonscheck et al., 2023) with a coarse spatial resolution of about 1.8° in the atmosphere, equaling a grid size of about 200 km. Second, we use 10 simulations of MPI-ESM1.2-HR (Müller et al., 2018), which has a spatial resolution of about 1.0° in the atmosphere, equaling a grid size of about 100 km. And third, we use a single realization of MPI-ESM1.2-XR (Gutjahr et al., 2019), which has 0.5° atmospheric horizontal resolution equaling a grid size of about 50 km. To quantify the time interval between two events of a given magnitude, we use return periods. We compare the return periods from the observed record of seasonal maximum daily precipitation in the respective regions with the simulations of different spatial resolution.

Realistically representing precipitation extremes depends on model spatial resolution

Our findings illustrate that the low-resolution MPI-GE CMIP6 is not able to simulate precipitation extremes as intense as the ones observed. However, the analyses show that the higher-resolution versions of the same model, MPI-ESM1.2-HR and MPI-ESM1.2-XR, capture the observed events much better. The extreme event in western Europe is captured by the single realization of MPI-ESM1.2-XR, which simulates a single daily summer precipitation as intense as the one observed with a more widespread but still similar pattern (Figure 4.2). The distribution of autumn daily maximum precipitation in the Western Alps is best represented by MPI-ESM1.2-HR. However, the magnitude of the observed extreme event on 2nd of October 2020 is within the range of the autumn daily maximum precipitation simulated by the mid-resolution version MPI-ESM1.2-HR and the high-resolution version MPI-ESM1.2-XR (Figure 4.2).

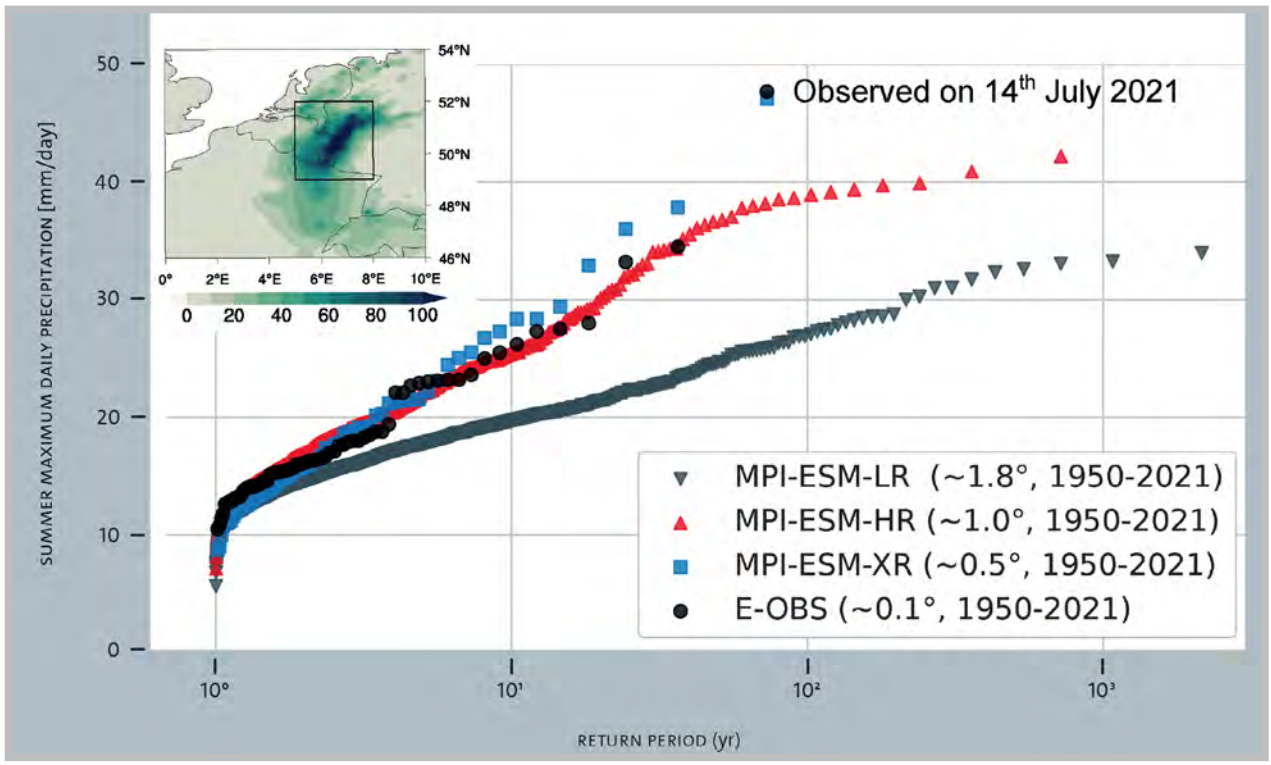

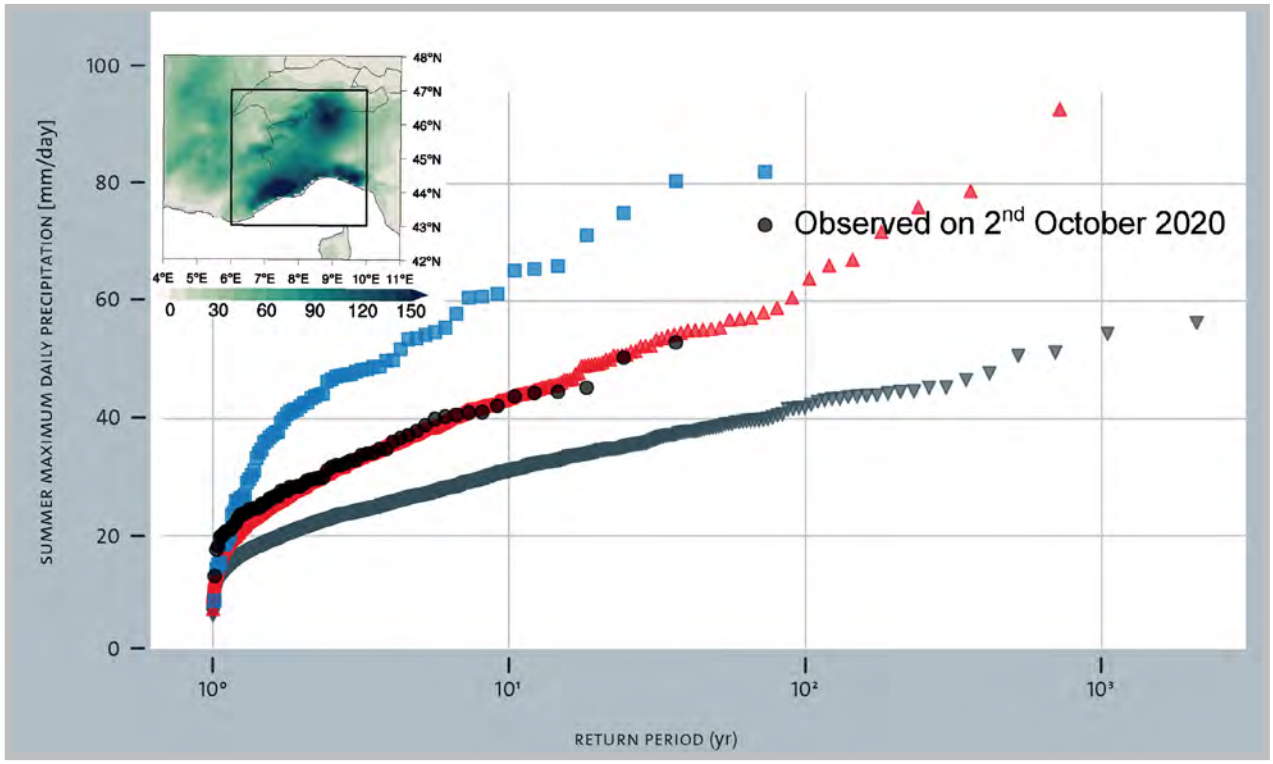

Figure 4.2: Representation of observed heavy precipitation extremes dependent on model spatial resolution: Return periods of (upper panel) summer (JJA) maximum daily precipitation averaged across the western European box, and (lower panel) autumn (SON) maximum daily precipitation averaged across the Western Alps box from 1950-2021 in three model resolutions from MPI-ESM1.2 and in observations. MPI-ESM-LR is based on 30, MPI-ESM-HR on 10, and MPI-ESM-XR and the E-OBS observations on only a single realization. Values of all summers or autumns and all realizations are merged for each ensemble (adapted from Olonscheck et al., 2023).

The finding that the higher-resolution simulations are able to capture the observed events is surprising because the spatial resolutions of 100 km and 50 km are insufficient to resolve important processes, such as moist convection. Our results suggest that the observed precipitation extremes investigated here are sufficiently large-scale to be represented by model simulations with 50 km or 100 km atmospheric resolution. We conclude that the available higher spatial resolution of MPI-ESM1.2 already substantially improves the representation of observed precipitation extremes, and that the required resolution strongly depends on the specific location and characteristics of the observed extreme event.

With the extreme event across the state of São Paulo, we push our model evaluation to the extreme case of comparing a locally measured precipitation amount to a spatial average of a model grid box. Our analyses show that the three different spatial resolutions of MPI-ESM1.2 are not able to simulate the observed magnitude and frequency of maximum summer precipitation measured in Mirante de Santana in São Paulo City. We find that higher spatial model resolution does indeed improve the simulation of both heavy precipitation magnitudes and frequencies. However, none of the three different resolutions is sufficient to represent the locally observed magnitude of summer heavy precipitation. This shows that local precipitation extremes cannot be captured by model simulations with grid sizes of 50 km and more because local topography is not accounted for, key physical processes are still parametrized, and local peaks of precipitation amounts are smoothed out by spatial averaging within a grid box.

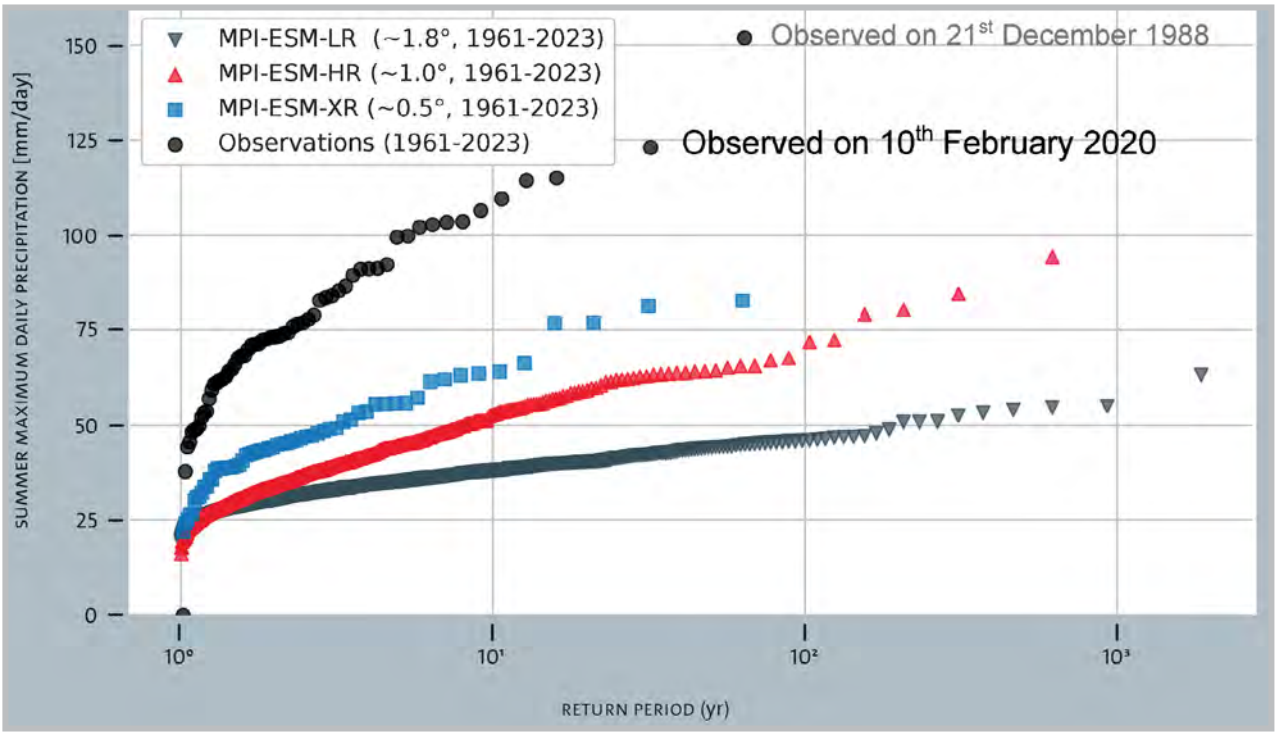

Figure 4.3: Representation of the heavy precipitation extreme observed in Mirante de Santana, São Paulo City, dependent on model spatial resolution. Return periods of summer (DJF) maximum daily precipitation averaged across the grid box that covers the measurement station Mirante de Santana at 23.5°S and 46.6°W in São Paulo City, Brazil, from 1961-2023 in three model resolutions from MPI-ESM1.2 and from the observed record (INMET, 2024). The weather station Mirante de Santana in São Paulo City is run by the National Institute for Space Research (INPE). Values of all summers (DJF for Southern hemisphere) and all realizations are merged for each ensemble. For comparison, the largest summer maximum precipitation on record, measured on 21st December 1988, is also labeled.

Consequences for adaptation

Constructing relevant and robust climate change information at the regional to local scale is key for integrated adaptation and mitigation planning and action (Revi et al., 2022). Climate models play an important role in providing a sound analytical basis for policymakers. Understanding the links between changes in extreme events and climate change and the impacts at local level is necessary for communicating the need for following ambitious adaptation pathways and thus effective local decision-making.

On top of climate change-induced increases in extreme precipitation events, other factors also determine the local impacts. For example, the current trend of urban development and further densification of urban areas toward increasingly impermeable surface fractions is expected to further

exacerbate the climate change-induced risk of flooding (Skougaard Kaspersen et al., 2017). In addition, urban development policies on flood control may even exacerbate flood risk due to adverse consequences of adaptation or mitigation responses (Dodman et al., 2022), in particular in terms of health and well-being implications (Quinn et al., 2023). Understanding the need for (urban) transformations requires further exploration of current and future climate-related hazards, exposure to these hazards, as well as the vulnerabilities at the local scale (Revi et al., 2023). However, such an assessment of regional to local climate change impacts requires knowledge of projections of climatic variables at a very fine scale, much finer than the one provided by global climate models so far (Slingo et al., 2022). Nevertheless, the current absence of local information on future extreme events from global climate models should not impede local action to adapt to already observed changes in extreme events.

Conclusions

We show that the resolution of state-of-the-art global climate model simulations is still too coarse to adequately represent locally measured heavy precipitation events, but that higher-resolution simulations of down to 50 km spatial resolution substantially improve the representation of observed extreme precipitation events compared to simulations with coarser resolution. We conclude that the ability of global climate model resolutions to represent observed record-shattering extreme events depends both on the model spatial resolution and on the specific characteristics of the observed heavy precipitation extreme (e.g., location, temporal/spatial scale, causal mechanism, type of precipitation, i.e., large-scale versus convective) (see also Sections 5.3, 5.4, and 5.5). Our findings reinforce the expected benefits from ongoing efforts in climate science to simulate the Earth at kilometer scale for a more sound representation of the Earth system. They confirm the urgent need for kilometer-scale global climate simulations to investigate the effect of climate change on small-scale extreme events, especially in the case of complex topography and short-duration convective events (Poschlod, 2022). Because of the substantial computational costs of kilometer-scale simulations, a trade-off between such high-resolution simulations and large ensembles (see Section 4.2) will be required for adequately capturing extreme precipitation events. Kilometer-scale simulations will be a big step forward for direct comparisons to locally measured extreme events, for increased trust in local future projections of extreme precipitation change, and for targeted adaptation actions.

4.4

High-Impact Marine Heatwaves

The global ocean has warmed substantially over the past decades. Concurrent with a long-term warming trend, episodic periods of anomalously high sea surface temperature at a particular location, known as marine heatwaves, are becoming more frequent, longer-lasting, more intense, and more extensive (Collins et al., 2019). Studies have documented a diverse range of local drivers (such as advection of heat by ocean currents or changes in air-sea heat fluxes) and large-scale modes (e.g., El Niño Southern Oscillation, Pacific Decadal Oscillation), along with teleconnections through internal processes such as Rossby waves (Li et al., 2020) that contribute to the generation and evolution of these events (Collins et al., 2019).

Over the past 25 years, at least 34 marine heatwave events globally have been associated with socio-economic consequences (Smith et al., 2021). Marine heatwaves have been shown to be responsible for dramatic mass mortality of marine mammals and iconic species (Smith et al., 2023), widespread coral bleaching (Sully et al., 2019), loss of Kelp Forest (Wernberg, 2021), depletion of seagrass meadows (Arias-Ortiz et al., 2018), and proliferation of harmful algal blooms (Trainer et al., 2020). In addition, they represent an immediate and pressing threat to the integrity of coastal carbon stocks (Serrano et al., 2021). Collectively, these impacts have global and regional socio-economic significance (see also Section 5.10).

Extreme climate-related events such as marine heatwaves exert direct effects on marine ecosystems and can also induce disturbances within the ecosystem, leading to prolonged impacts that extend beyond the event's duration (Bastos et al., 2023). For instance, 36% of Shark Bay's seagrass meadows in Australia, which support the largest seagrass carbon stocks worldwide, were damaged following a marine heatwave in 2010/2011 (Arias-Ortiz et al., 2018). This damage could potentially lead to the release of CO_2 into the atmosphere over the subsequent years. Of significant concern are compound extreme events. For example, marine heatwaves coinciding with ocean acidity extremes (Burger et al., 2022) or extreme sea level (Han et al.,

2022) can lead to severe ecosystem service-related impacts that human societies depend upon.

In this section, we discuss the evolution of high-impact marine heatwaves across four case studies, focusing on regions at an especially high risk of increased severity in marine heatwaves. The vulnerable regions include the Mediterranean Sea as well as the Indian, Northeast Pacific, and Arctic Oceans. Their vulnerability arises from a combination of factors such as biodiversity hotspots, presence of species which hold ecological and commercial significance and/or face the threat of extinction, highly populated coastal communities that rely significantly on marine ecosystem for their livelihood, and other factors (Smale et al., 2019). In the case studies of the Arctic and the Northeast Pacific, we also present results on the extent to which greenhouse gas forcing has contributed to the severity of these events. Finally, we discuss why clear definitions of marine heatwaves are essential to enable coastal communities to adapt effectively.

The evolution of high-impact marine heatwaves

To identify marine heatwaves, we use the daily Optimum Interpolated Sea Surface Temperature (OISST) satellite data set at a resolution of 0.25° × 0.25°, for the period between the years of 1982 and 2022 (Reynolds et al., 2007). We define marine heatwaves as occurring when sea surface temperatures exceed a seasonally varying threshold, here the 95th percentile of sea surface temperature variations based on a 30-year climatological period (1983–2012), for at least five consecutive days.

In the case studies of the Arctic and the Northeast Pacific, we also discuss the extent to which greenhouse gas forcing has contributed to the severity of these events, based on data from Barkhordarian et al. (2022; 2024). We employ an extreme-event attribution technique and use daily sea surface temperature output from the NCAR CESM-LE (Kay et al., 2015), which provides large-ensemble members with fixed greenhouse gas forcing. We estimate the probabilities of marine heatwaves with specific characteristics (duration, intensity, and cumulative heat intensity) occurring in the presence and absence of greenhouse gas forcing. These probabilities are calculated for both actual (all-forcing includes anthropogenic and natural external forcing) and counterfactual (fixed greenhouse gas forcing) scenarios, using observations as threshold and model simulations. The estimated probabilities are used to calculate event-attribution metrics.

Northeast Pacific – the deadly "blobs"

During the decade between 2012 and 2022, the sea surface temperatures over the Northeast Pacific were the warmest ever recorded, characterized by the occurrence of extreme marine heatwaves known as deadly "warm blob" events. Among other impacts, these marine heatwaves caused dramatic mass mortality events in seabird species and major outbreaks of harmful algal blooms that produce extremely dangerous toxins (Smith et al., 2023). Barkhordarian et al. (2022) show that the Northeast Pacific warming pool is marked by concurrent and pronounced increases in the annual mean and variance of sea surface temperature, decreases in wintertime low-cloud cooling effect, and increases in atmospheric stability. Consequently, the greater exposure to heat and the lack of usual wintertime cooling leads to 4.5-fold more frequent, ninefold longer-lasting, and threefold more intense marine heatwaves in the past decade (2012-2022), in comparison with those occurring in the previous decades.

According to the study by Barkhordarian et al. (2022), based on OISSTv2 satellite data, up to 60% of the marine heatwaves detected in the Northeast Pacific over the past decade are either more intense and/or longer-lasting than could solely be attributed to internal climate variability in the absence of external climate drivers. Extreme-event attribution analysis presented in the paper further reveals that greenhouse gas forcing has virtually certainly (with > 99% probability) caused the multiyear persistent 2014-2015 and 2019-2021 marine heatwaves, in terms of both intensity and duration.

Arctic Ocean and its marginal seas

OISSTv2 satellite data reveals that the summer of 2007 was the beginning of a shift toward a new era of marine heatwaves over the shallow marginal seas of the Arctic Ocean. Barkhordarian et al. (2024) show that marine heatwaves in the Arctic are primarily triggered by an abrupt retreat of sea-ice, coinciding with the midsummer peak of downward radiative fluxes. In terms of frequency, an extreme marine heatwave with 140°C cumulative heat intensity (the integral of sea surface temperature anomalies over time for the duration of the event), which is a one-in-40-years event in a world without greenhouse gas forcing, turns into a one-in-5-years event under the influence of greenhouse gas forcing.

By utilizing an extreme event-attribution technique, Barkhordarian et al. (2024) demonstrate that any marine heatwave event over the shallow marginal seas of the Arctic Ocean with an intensity larger than 1.5°C has a less than 1% occurrence probability under no-greenhouse gas effect. Thus, for extreme marine heatwaves, such as those of 2007 with 3.5°C intensity and those in 2020 with 4°C intensity, greenhouse gas forcing is virtually certainly the cause. The study further shows that if greenhouse gas forcing continues to rise, along with the expansion of first-year ice extent, moderate marine heatwaves will very likely persistently reoccur. These changes are expected to have far-reaching consequences for global climate dynamics and the well-being of Arctic ecosystems and communities.

Mediterranean Sea

Despite its relatively small size, the Mediterranean Sea is known for its remarkable biodiversity and serves as a significant reservoir of marine species, representing between 4% and 18% of the total global marine species richness (Coll et al., 2010; Würtz, 2010). Our analysis, based on OISSTv2 satellite data, shows a rapid and non-linear escalation in the number of marine heatwave days in the region. In the western, central, and Adriatic basins, marine heatwaves are related to increased incoming solar radiation, along with reduced ocean heat losses, possibly due to warm and humid air intrusions (Simon et al., 2023). From 1982 to 2010, the region experienced an average of 15 marine heatwave days per year. However, between 2011 and 2022, this count has quadrupled, reaching an average of 70 marine heatwave days per year. As background sea surface temperature has increased linearly between 1982 and 2021 by 0.38°C per decade, corresponding to about three times the global ocean warming rate, the number of marine heatwave days does not follow a linear pattern but instead exhibits a non-linear response (Figure 4.4, upper panel).

This substantial and accelerated rise in marine heatwave occurrences highlights the escalating thermal stress experienced by the Mediterranean ecosystems and contributes, at least in part, to the onset of five consecutive years of widespread mass mortality events between 2015 and 2019 across the basin (Garrabou et al., 2019; 2022).

Indian Ocean (Maldives)

The Maldives are an archipelago in the Indian Ocean composed of 26 atolls surrounded by coral reefs, which provide habitat for a diverse array of marine life and play a crucial role in sustaining the local economy and society (Stojanov et al., 2017; Sully et al., 2019; see also Section 5.10). The Maldives have experienced several instances of coral-bleaching events triggered by marine heatwaves in recent years (Perry and Morgan, 2017; Shlesinger and van Woesik, 2023). In the Indian Ocean, the positive phase of the El Niño Southern Oscillation and the Indian Ocean Dipole mode are the dominant large-scale modes to influence marine heatwave occurrence (Holbrook et al., 2020). Strong El Niño years, such as 1997-1998, 2015-2016, and, to a lesser extent, 2009-2010, are clearly evident as peaks in the average number of marine heatwave days, with hotspots over the Arabian Sea and the western equatorial Indian Ocean (Figure 4.4, lower panel).

The non-linear amplification of marine heatwave days, which are generally considered representative for chronic heat stress exposure (Smale et al., 2019), signifies a shift in the region's thermal conditions that leads to mass coral-bleaching events. Coral bleaching poses a significant threat to marine ecosystems due to the critical role coral reefs play in preserving biodiversity, sustaining fisheries, and offering coastal protection (Shlesinger and van Woesik, 2023).

Precise definitions of marine heatwaves play an important role in effective adaptation for coastal communities

The most commonly used definition for marine heatwave has been developed by Hobday et al. (2016), who describe a marine heatwave as "a discrete prolonged anomalously warm water event". The question is: "What is anomalous"? The term "marine heatwave" can encompass two distinct interpretations: (1) it could refer to an extreme heat relative to historical temperature records, thus signifying relative heat; (2) it could refer to an extreme heat relative to an evolving "new normal" of rising temperature owing to climate change, signifying absolute heat.

As discussed by Amaya et al. (2023), a fixed baseline, which measures heat relative to historical temperature and thus characterizes "total heat exposure"—the combination of gradual temperature increase and short-term heat events—is useful when monitoring events like coral bleaching. Marine species with short life cycles may have some ability to adapt to gradual temperature increase, but they might not necessarily cope well with rapid heat shocks. By contrast, some corals may recover from immediate heat shocks but struggle with prolonged exposure to heat (Provost and Botsford, 2022). While the relative heat metrics has its merits, it fails to consider the underlying factor of climate change causing a gradual increase in ocean temperatures over time. By contrast, defining marine heatwaves relative to gradually increasing temperatures enables resource managers to differentiate between temporary fluctuations and long-term trends. For instance, the fishing industry could temporarily suspend fishing to manage a rapid heat shock. Adapting to prolonged warming may necessitate actions such as relocating to different fishing grounds, and/or targeting alternative species (Fisher et al., 2021).

Thus, different baselines (measuring absolute or relative heat) results in different interpretations of frequency, intensity, and duration of marine heatwaves. These would lead to varied outlooks and emphasizes the importance of accurate information for informed decision-making (Amaya et al., 2023).

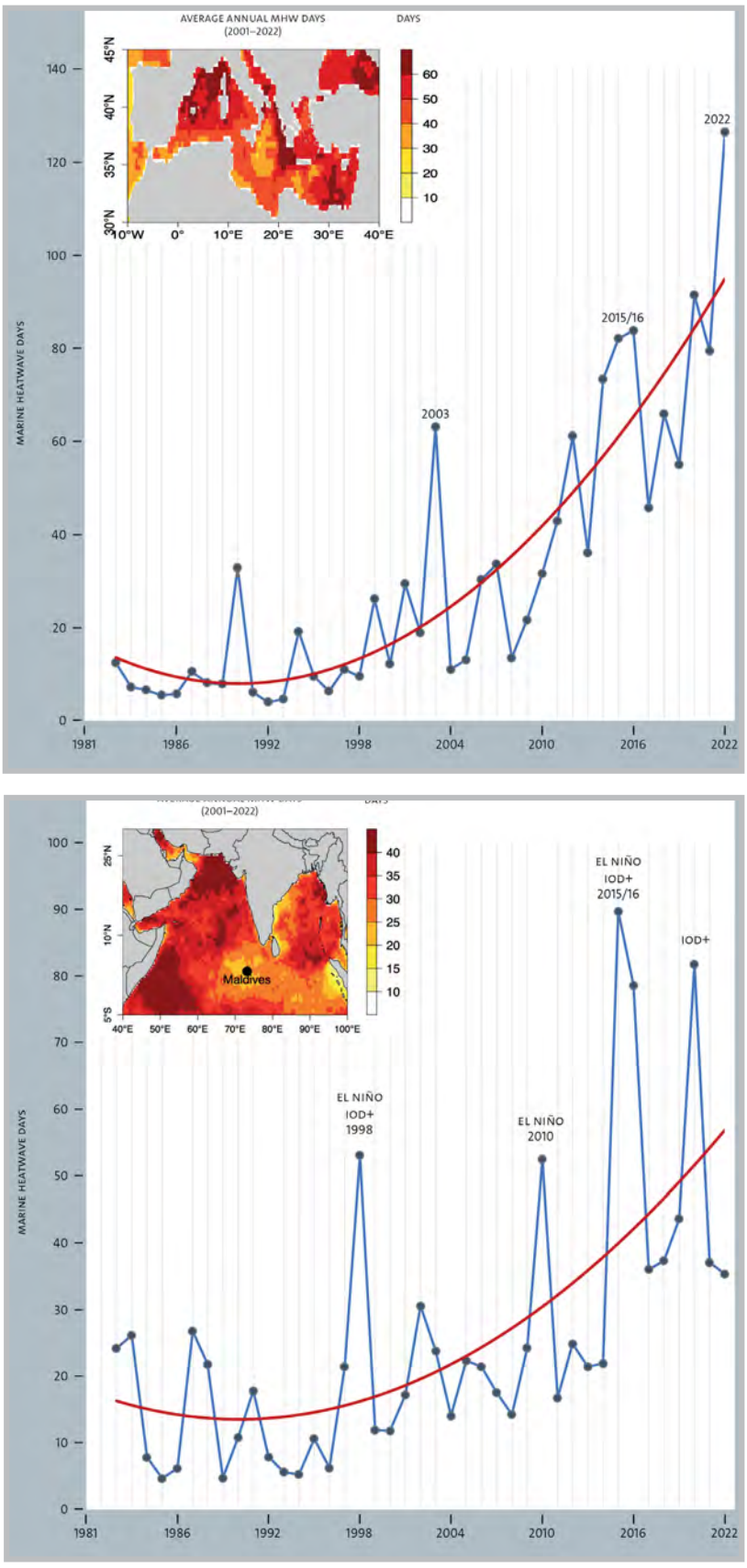

Figure 4.4: Time series of annual marine heatwave days between 1982 and 2022 over the Mediterranean Sea (upper panel) and the Indian Ocean (lower panel). IOD+ refers to the positive phase of the Indian Ocean Dipole mode. Red curves represent quadratic regression.

Conclusions

This section offers a worldwide view of the trends, impacts, and attribution of marine heatwaves, particularly focusing on four regions especially at high risk of increased marine heatwave severity. The accelerated (non-linear) increase in marine heatwave occurrences across vulnerable regions such as the Mediterranean Sea and the Indian Ocean underscores the escalating thermal stress on marine ecosystems that has resulted in significant impacts, including mass coral bleaching events across the Indian Ocean (Shlesinger and van Woesik, 2023) and five consecutive years of widespread mass mortality events between 2015 and 2019 across the Mediterranean Sea (Garrabou et al., 2019; 2022; see also Section 5.10). Over the Northeast Pacific, up to 60% of the high-impact marine heatwaves detected over the past decade are more severe than could solely be attributed to natural climate variability in the absence of external climate drivers (Barkhordarian et al., 2022). Over the Arctic Ocean, abrupt sea-ice retreat in the shallow marginal seas during the maximum of downward radiative flux has led to unprecedented marine heatwaves that have become much more likely as a result of greenhouse gas forcing (Barkhordarian et al., 2024). In summary, marine heatwaves, which are very likely to become more frequent and more intense due to human-induced emissions (Collins et al., 2019), cause extensive damage to marine ecosystems and the coastal communities that rely on them for goods and services. This highlights the importance of effective strategies for adaptation.

4.5

How Will Extreme Heat in the World's Breadbasket Regions Change in the Future?

A key challenge in adapting to anthropogenic climate change is ensuring food security. Understanding how food supply through agriculture may change under climate change is paramount to addressing this challenge. Extreme climate events such as heatwaves and droughts that occur in several regions in the same year may exacerbate potential crop yield losses (Raymond et al., 2022) and lead to individual years of extremely low yields if multiple important crop production regions, so-called *breadbasket regions*, are hit. Here, we take a climatic perspective to this problem and analyze how the likelihood of several breadbasket regions that together account for more than 55% of global maize production (Gaupp et al., 2020) experiencing a heatwave during the same maize growing season may change at 1.5°C and 2°C of global warming compared to pre-industrial climate.

There is extensive literature on the relationship between agricultural yields and climate (e.g., Lobell et al., 2011; Rosenzweig et al., 2014). Studies generally find effects of extreme temperature (Luo, 2011) and drought (Doorenbos and Kassam, 1979) on agriculture, emphasizing a strong combined effect of heat and drought for maize (Gaupp et al., 2020). Heat and drought affect the development of the plants during their growing season, which is typically in summer (Gaupp et al., 2020). As a first step toward projecting the changes in maize crop yields due to such threats, we here examine heat extremes. These may impact maize production by reducing the number of flowers, impairing pollen tube development during plant growth, and limiting pollen release and fertility during the plants' reproduction phase (e.g., Teixeira et al., 2013), or impairing the productivity of agricultural workers (de Lima et al., 2021; Orlov et al., 2021). These impacts may only partly be mitigated by irrigation of the crops (Siebert et al., 2017).

Previous work on projected changes of crop yields considered mean changes by the end of the 21st century (Franke et al., 2020; Jägermeyr et al., 2021). Such assessments showed conflicting results, but generally illustrated a global decrease of crop yields for maize (Jägermeyr et al., 2021). However, natural climate variations may also substantially affect regional and global crop yields, on at least two-thirds of the global cropland area (Heino et al., 2018). These variations are partly reflected in current crop yield projections as uncertainties in the end-of-century estimate (Jägermeyr et al., 2021) but are not considered explicitly, which hampers the representation of extreme climate events in crop yield projections.

Extreme events in the climate system are projected to change under global warming (Field et al., 2012; Suárez-Gutiérrez et al., 2020; Patterson, 2023). Heat extremes, for example, may change in

their intensity, duration, and spatial extent, or even compound with further extremes such as droughts, exacerbating their impact (Zscheischler et al., 2018). Hot and dry compounds are not strictly separable since heat may drive increased evaporation that dries out the soils and plants, exacerbating further heating (e.g., Zscheischler et al., 2018). Extremes may also compound in time or space, meaning that long time periods or large areas may be affected by an extreme, again increasing their impact. As discussed above, such extremes may be detrimental for agricultural crop yields both locally and on a large scale, particularly in vulnerable communities. Taken together, these factors lead to the question of how extreme heat in areas with vulnerable communities as well as in the world's breadbasket regions may change under global warming.

An example of a region that is susceptible to agricultural disruption is rural northern Namibia: Communities there are heavily dependent on subsistence farming and are therefore particularly vulnerable to climate extremes that challenge crop production and may disrupt local food security. We analyze such a disruption of crop production here as a case study, while a case study in Section 5.8 addresses a further challenge of rural Namibia, namely the adaptation of pastoralists to climate change.

Raymond et al. (2022) used the MPI-GE CMIP5 to address the impact of extreme climate events on important maize production regions. They found that global warming increases the likelihood for hot-dry compound events to occur in several of these regions both individually (by 100-300%) and during the same growing season, indicating increased risk to the global food system. In this context, extremes in multiple of these breadbaskets may be teleconnected through atmospheric processes (Kornhuber et al., 2020; Meehl et al., 2022).

These studies leave the expected change of extreme events at different levels of global warming to be examined. Specifying the probability of extreme events according to global warming levels will not only be a useful policy tool to motivate mitigation efforts but can also inform the planning of adaptation strategies to ensure food supply under global warming. As a first step in this direction, we outline here the change of extreme heat events in the breadbasket regions at 1.5°C and 2°C of global warming compared to pre-industrial climate.

Analyzing compound heat extremes in crop-growing regions

We first analyze extreme heat at different levels of global warming in the crop growing regions of Northern Namibia as an example of a region with vulnerable subsistence farming communities. Second, we consider heatwaves in multiple breadbasket regions around the world during the same growing season. A basic assumption in our analysis is the lack of adaptation to increasing extreme events through the cultivation of better adapted crops so that our results represent an upper bound of potential impacts.

We apply the most recent version of the MPI-GE (see Section 4.2) because it allows for a thorough and representative analysis of climate extremes due to the large sample size (e.g., Bevacqua et al., 2023; Olonscheck et al., 2023). Global warming levels are identified for all ensemble members under the SSP2-4.5 scenario of the MPI-GE CMIP6 separately. This entails evaluating 30-year-intervals centered around the time global mean temperature first crosses the 1.5°C and 2°C warming levels with respect to the 1850–1900 mean.

A day is classified as extreme if its maximum temperature exceeds the threshold set by the top 5% of maximum temperatures across all ensemble members during the period of 1990 to 2020 for the corresponding calendar day. We then define a heatwave using spatial and temporal compounding, like in Raymond et al. (2022): If at least one-third of the area of the examined region is affected by a heatwave for more than three days in a row during the growing season, a heatwave is recorded for this region.

Projected heat extremes in one region—the example of northern Namibia

We illustrate the probability change of heat extremes under global warming using the example of northern Namibia. Low crop productivity is a pervasive problem in smallholder farming systems across Sub-Saharan Africa, primarily due to declining soil fertility, inadequate access to fertilizers, and climate extremes (Wall et al., 2013). In Namibia, rainfed agricultural production is constrained to the northern and north-eastern regions, where smallholder farms dominate and face challenges such as low crop yields and underdeveloped market chains and food processing. Traditionally, smallholders in this region have limited access to chemical fertilizers, manure, or other inputs, despite soil analyses indicating that sandy and low-fertility soils limit crop productivity (de Blécourt et al., 2019). Legumes play a crucial role in overcoming this limitation as they do not rely on mineral nitrogen, are relatively drought-resistant, and grow in low-fertility sandy environments (Vanlauwe et al., 2019; Becker et al., 2023). Furthermore, they provide nutrient-rich, high protein foods and are already a prominent food crop in Southern Africa (Vanlauwe et al., 2019; Rasche et al., 2023). Here, field studies have revealed that the optimal temperature for legume cultivation is often exceeded during the growing season (De Notaris et al., 2020). Measurements in northern Namibia have shown that soil surface temperatures already regularly exceed 35°C (SASSCAL Weathernet, 2024), surpassing the optimal temperature for plant growth and rhizobial nodulation, which results in reduced crop weight and number (Marsh et al., 2006;

Bhandari et al., 2017). Physical connections between heat and drought through increased evaporation (e.g., Trenberth and Shea, 2005) and interconnections between dry soil and heat (e.g., Seneviratne et al., 2010) can further exacerbate heat wave impacts on crop productivity in water limited regions. Increasing heat stress could thus limit a major protein source for local communities while also hindering potential adaptation strategies.

We used December until February as crop growing season in northern Namibia. During the period between 1990 and 2020, 2-7% of growing seasons experience heatwaves in the model (Figure 4.5). This means that heatwaves cover between 2% and 7% of the growing seasons in the different ensemble members (for "ensemble spread of probability", see Section 4.2). This result is expected since the 95% extreme threshold was defined based on this same time period. With 1.5°C and 2°C of global warming, the likelihood for a heatwave to occur is projected to increase from 5-14% and 10-22%, respectively (Figure 4.5). This means that in the MPI-ESM-LR Earth system model, extreme heat affects at maximum 14% of the growing season in northern Namibia if 1.5°C of global warming are reached. If the Paris Agreement temperature goals are breached and 2°C of global warming are reached, a heatwave on 10% of all days of the growing season is virtually certain in northern Namibia, and heatwaves may cover as much as 22% of the growing season. By the end of the century, a period characterized by around 2.25°C of global warming under the SSP2–4.5 scenario, 15-26% of days of the growing season experience a heatwave in our model.

Our findings illustrate the urgent need to mitigate any degree of global warming and highlights adaptation potential by preparing for a more frequent occurrence of extreme soil surface temperature.

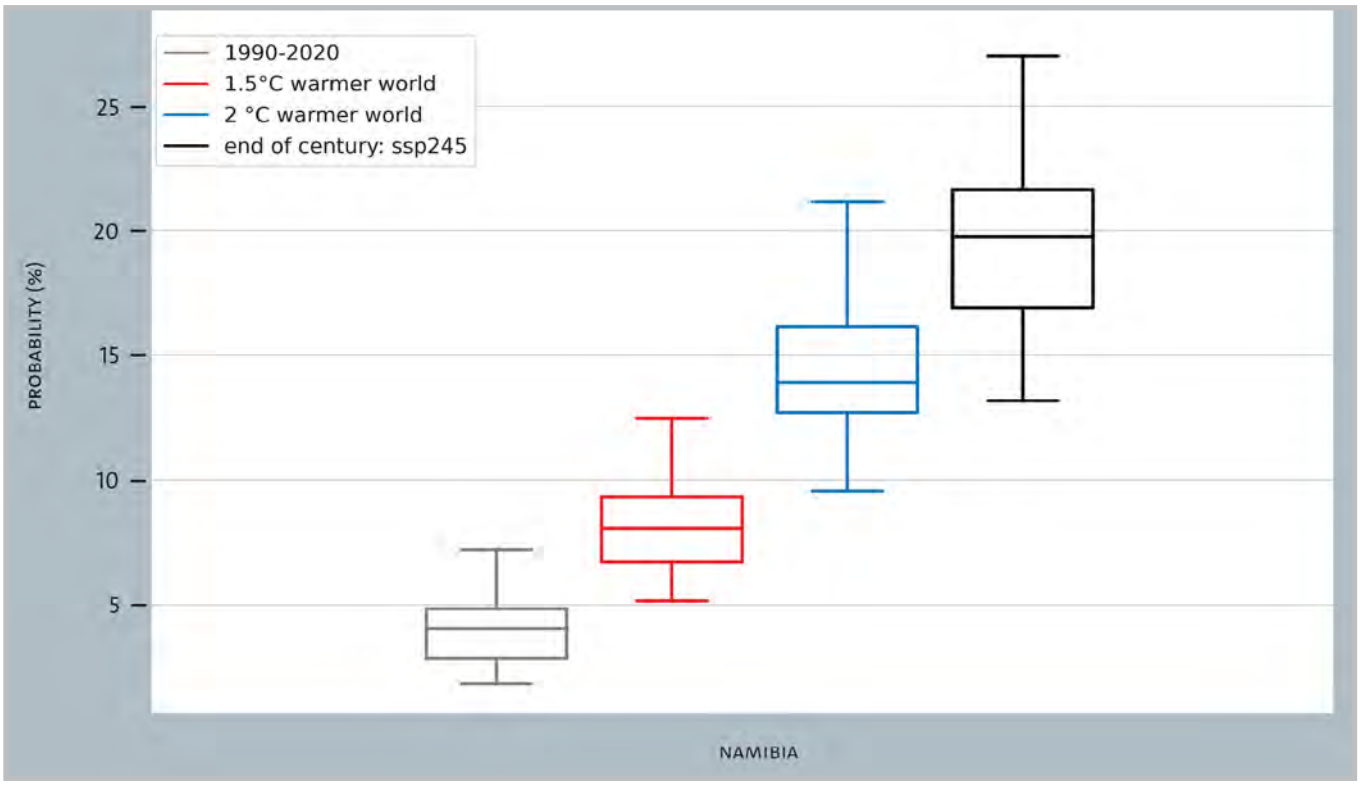

Figure 4.5: Ensemble probability for a heatwave to occur in Northern Namibia during the growing season, evaluated for the periods of 1990 to 2020 (gray) and 2070 to 2100 (black), as well as under 1.5°C (red) and 2°C (blue) of global warming. The future information is based on climate projection simulations with the MPI-ESM-GE CMIP6 under the SSP2-4.5 scenario.

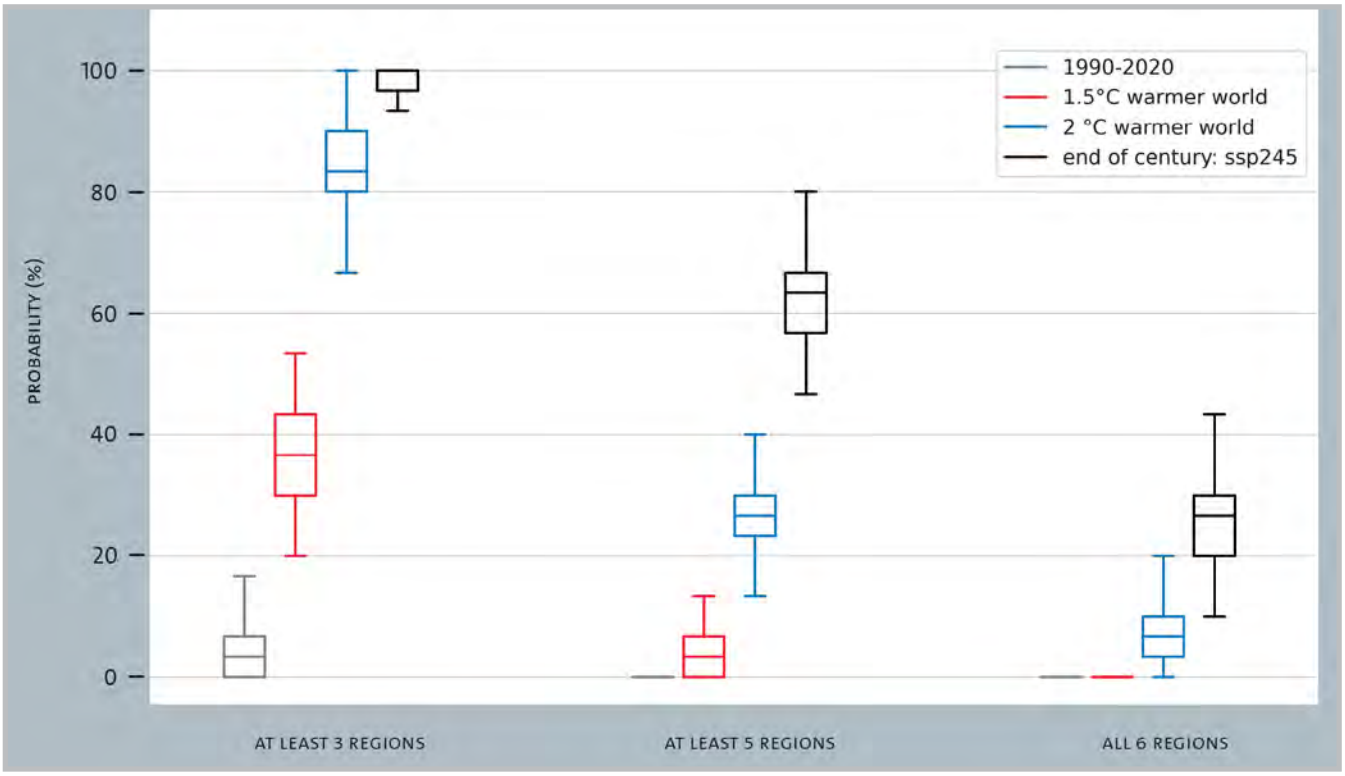

Figure 4.6: Ensemble probability for a heatwave to occur during the same maize growing season in at least 3, 5, or all 6 breadbasket regions, evaluated for the periods of 1990 to 2020 (gray) and 2070 to 2100 (black), as well as under 1.5°C (red) and 2°C (blue) of global warming. The future information is based on climate projection simulations with the MPI-ESM-GE CMIP6 under the SSP2–4.5 scenario.

Heat extremes in multiple breadbasket regions during the same growing season

Increasing global warming in the presence of internal climate variability not only increases the risk that individual regions experience a heatwave; it also increases the risk that several regions experience a heatwave during the growing season of the same year. To explore this risk, we now consider heatwaves in several breadbasket regions during the same growing season. Note that while 30 ensemble members used here are likely enough to accurately represent internal variability and thus heat extremes in individual regions (Milinski et al., 2020), capturing a compounding between multiple regions might require a larger ensemble. A detailed analysis of this effect is beyond the scope of what can be achieved here and thus left for a future study. We focus our analysis on the breadbasket regions used in Raymond et al. (2022), which are: Central North America, North-East Brazil, southern South America, Central Europe, East Asia, and South Asia, as defined in the IPCC Special Report on Extremes (IPCC, 2012). In these different regions, different growing seasons for the crops are considered. These are: May until November in Central North America, December until February in North-East Brazil and South South America, May until August in Central Europe, May until September in East Asia, and July until October in South Asia. A simultaneous extreme event in several of these regions may substantially impact crop yields, disrupting local and global food markets and jeopardizing food security (Raymond et al., 2022). We thus examine whether heatwaves compound between regions. To this end, the share of the six breadbasket regions affected by a heatwave during the same growing season (southern hemisphere summer preceding northern hemisphere summer) is calculated for every ensemble member. This yields the number of regions that experience a heatwave during the same harvest year, potentially affecting global cereal prices and food security, which could be avoided through further process understanding and careful adaptation to these kinds of events.

The risk for a heatwave to occur in at least three breadbasket regions at the same time has historically ranged from 0-7% (Figure 4.6). Assuming 1.5°C of global warming, such an event may occur in up to 50% of years, while 2°C of global warming increase the risk of a three-region-event to between 62% and 97%. By the end of the century, a three-region-event is projected to occur every year under the SSP2–4.5 scenario.

At present, heatwaves do not affect five or more breadbasket regions during the same growing season (Figure 4.6). This changes under global warming, when the probability reaches up to 7% at 1.5°C,

between 12% and 42% at 2°C of global warming, and between 42% and 80% by the end of the century. These values highlight both the pronounced uncertainty that still exists in these estimates and the strong increase in extreme event exposure of maize crops with every additional increase in global warming. The interplay of anthropogenic climate change and internal climate variability alongside spatial and temporal compounding of extremes is characterized by numerous non-linearities that together may lead to profound potential impacts on our food system and society. Probabilities of all six breadbasket regions experiencing a heatwave during the same growing season underline this finding: While such events are not found under present climate conditions or 1.5°C of global warming, heatwaves occur in all six regions up to 19% of years at 2°C of global warming and reach probabilities of 10-40% by the end of the century.

Conclusions

This case study highlights how the interplay of non-linearities in the climate system that involve internal climate variability may exacerbate the impacts of anthropogenic climate change with potentially devastating consequences. Extreme events may compound in space and time (occur in quick succession or in several regions at once), which may increase the severity of their impacts. Agricultural systems, if left unmanaged, are particularly vulnerable to such extremes, which already now has pronounced impacts on society. Synchronized climate events, such as heat extremes that hit several breadbasket regions during the same growing season, pose an additional risk to global food security and supply chains (e.g., Mehrabi, 2020) that may particularly strongly impact import-dependent regions (Puma et al., 2015). Meanwhile, climate models underestimate the physical mechanisms that synchronize extreme events (Kornhuber et al., 2023). Therefore, on the one hand, the results presented here can be understood as a lower bound to the threats that climate change poses to food security. On the other hand, studies have shown that trade and storage of food can act as powerful buffers to mitigate impacts of climate extreme induced agricultural losses (e.g., Molina Bacca et al., 2023). Our findings underline the urgent need for rapid and effective mitigation of climate change. Since some of the extreme events considered here already occur at an increased likelihood, decision-makers, including individual households and subsistence farmers (Petzold et al., 2023a), should also consider efforts to prepare adaptation measures to these kinds of extremes, for example by mitigating short-term impacts on the agricultural sector through the establishment of irrigation systems (Siebert et al., 2017) or changes in crop variety.

4.6

Summary

Attribution studies have shown high confidence that anthropogenic climate change has increased the likelihood and intensity of extreme events. However, the power of (decadal) internal climate variability should not be underestimated. It can turn events that are currently considered extreme and that are expected to be normal at the end of the century due to global warming into events that are plausible to occur already within the next 20 years (Section 4.1). The assessments in Sections 4.3, 4.4, and 4.5 emphasize the need to explicitly consider internal climate variability in models to improve the understanding and the quantification of projected changes in extreme events. Especially the interplay between anthropogenic climate change and internal climate variability involves non-linearities that can amplify or attenuate changes in climate extremes on a regional scale. The outcome of the assessments reveals three aspects relevant for assessing the plausibility of adapting to climate change in a sustainable manner.

First, knowing the uncertainties and limits of climate models is key for assessing the quality of the observed extreme events' representation, and, in a second step, for predicting future extreme events. This, in turn, is crucial for setting effective and sustainable climate adaptation measures. Section 4.3 on precipitation extremes offers an insightful example. Here, both internal variability and coarse model resolution are challenges for producing realistic representations. The assessment shows two main points: First, that large-ensemble simulations with increased spatial resolution substantially improve the representation of the investigated precipitation extremes, and second that the required spatial resolution strongly depends on the specific location and characteristics of the extreme event. The outcome is that not all model simulations are fit for the purpose of providing high-quality information for adaptation. This has implications for affected communities planning adaptation measures to precipitation extremes and the following floodings, such as

communities in water-scarce regions, regions with riverine systems or steep topography, and cities such as Hamburg and São Paulo (Section 5.3 and 5.4).

Second, while communities have to react to extreme events—no matter if they occur because of anthropogenic climate change or internal climate variability—, for the planning and development of climate change adaptation strategies, knowing what a community is adapting to is crucial. Attribution studies analyze to what extent high-impact events can be attributed to anthropogenic climate change or to internal climate variability. Thus, in the Outlook terminology, the field of extreme event attribution engages in identifying the driving forces that regulate the physical boundary conditions for society. This requires a sophisticated view on extreme events, considering that "extreme" means different things in different situations. Section 4.4 describes an attribution study and highlights the dominant role of anthropogenic climate change in the occurrence of extreme events. For example, marine heatwaves with an intensity larger than 1.5°C have less than 1% occurrence probability without greenhouse gas forcing, but the Arctic Ocean experienced marine heatwaves with 3.5°C and 4°C intensity in 2007 and 2020, respectively. Thus, for both events greenhouse gas forcing is virtually certainly the cause, in a necessary causation sense. In terms of frequency, an event that is a one-in-40-years event in a world without greenhouse gas emissions turns into a one-in-five-years event with greenhouse gas emissions (Section 4.4).

Third, the assessments in Section 4.3, 4.4, and 4.5 emphasize that the interplay of non-linearities can lead to ecosystem and socio-economic disruptions, with potentially devastating consequences. Compound extreme events can become particularly dangerous. Section 4.5 assesses the change in the probability of compound extreme heatwaves with increased warming and the implications for cropland areas. The probability that extreme heatwaves occur in three breadbasket regions during the same year increases from a historical 0% to 7%, to 50% at 1.5°C global warming, to between 62% and 97% if the Paris Agreement temperature limit is breached and 2°C of warming are reached, to one event every year at about 2.25°C of global warming by the end of the century (Section 4.5). In a potential combination with concurrent dry spells (Raymond et al., 2022), such events may cause crop-yield losses with impacts on local and global cereal prices and supply chains, resulting in threats for food security. While studies indicate that trade and storage may buffer shocks to the food system to some degree (Molina Bacca et al., 2023), the spatially compounding nature of the studied heat events poses new challenges to constructing a climate-resilient food system. Also, precipitation extremes and severe floodings are among the most devastating and costly events, damaging infrastructure, private property, and even causing fatalities (Section 4.3). Marine heatwaves are powerful catalysts of ecosystem disruption (Section 4.4). Being responsible for escalating thermal stress experienced by ecosystems, mass mortality, coral bleaching, and Kelp Forest loss, marine heatwaves disrupt the delivery of marine ecosystem goods and services to coastal communities that rely on them, and beyond that have an impact on economy and coastal protection needs against increased erosion (see Section 5.10).

Authors: Anna Pagnone, Jochem Marotzke

4.1: **Jochem Marotzke,** Anna Pagnone

4.2: **Dirk Olonscheck**, Leonard Borchert, Adrien Deroubaix

4.3: **Dirk Olonscheck,** Franziska S. Hanf

4.4: **Armineh Barkhordarian**

4.5: **Leonard Borchert,** Victoria Dietz, Joscha N. Becker, Kerstin Jantke

4.6: **Anna Pagnone**